Self-Organized Nanoscale Pattern Formation on Vicinal Si(111) Surfaces via a Two-Stage Faceting Transition

F. K. Men,[1,*] Feng Liu,[2] P. J. Wang,[1] C. H. Chen,[1] D. L. Cheng,[1] J. L. Lin,[3] and F. J. Himpsel[3]

[1]*Department of Physics, National Chung Cheng University, Chia-Yi, Taiwan, Republic of China*
[2]*Department of MSE, University of Utah, Salt Lake City, Utah 84112*
[3]*University of Wisconsin–Madison, Madison, Wisconsin 53705*
(Received 7 July 2000; revised manuscript received 4 December 2001; published 15 February 2002)

We demonstrate a self-organized pattern formation on vicinal Si(111) surfaces that are miscut toward the $[\bar{2}11]$ direction. All the patterns, consisting of a periodic array of alternating (7×7) reconstructed terraces and step-bunched facets, have the same periodicity and facet structure, independent of the miscut angle, while the width of the facets increases linearly with miscut angle. We attribute such unique pattern formation to a surface faceting transition that involves two transition stages: the first stage forms a stress-domain structure defining the universal periodicity; the second stage forms the low-energy facets controlling the facet width.

Surface patterning is an important processing step in many device fabrication processes. The continued drive to make devices smaller and smaller has brought up the challenge to pattern surfaces in the nanometer scale where conventional lithographic techniques are no longer applicable. Two different routes have been taken toward nanopatterning: one by developing new patterning techniques with nanometer resolution, such as scanning probes, the other by taking advantage of self-organization of surface patterns occurring naturally. The latter approach has shown great promise because it offers an economic and parallel process for device fabrication.

Surface stress often plays an important role in driving surface structural and morphological ordering, in particular, through the surface stress-induced spontaneous formation of ordered patterns of stress domains [1]. An effective way to create the stress-domain patterns is by step motion and/or by surface faceting transition on vicinal surfaces, as demonstrated on a variety of surfaces, such as the Si(001) [2], Si(111) [3–5], GaAs(001) [6], Au(111) [7], and Pt(001) [8] surfaces.

Ideally, one would like to create a desirable surface pattern with controllable length scales. The characteristic length scales of the stress-domain patterns are generally determined by the competition between elastic relaxation energy and domain boundary energy. Therefore, in principle, it should be possible to control the length scales of such patterns by manipulating these energy terms. However, such control is difficult to achieve in practice. For example, the size of stress domains can be changed by applying external strain [2], but the domains restore their original size upon relieving the external strain. On a vicinal surface the terrace size can be changed by tuning a miscut angle, but different step structures [9,10] and facets [5] usually form at different miscut angles.

In this Letter, we demonstrate the possibility of creating the same surface pattern of controllable nanometer length scales. We show that when the Si(111) surfaces are miscut toward the $[\bar{2}11]$ direction, thermal annealing leads to formation of one-dimensional surface patterns consisting of a periodic array of alternating flat terraces and high-step-density facets, with very good long-range order. Most importantly, all the surface patterns exhibit the same atomic structure for both the terraces and the facets and the same periodicity, independent of miscut angle, while the width of the facets increases linearly with increasing miscut angle. We propose that such unique self-organized pattern formation is achieved by a surface faceting transition that involves two transition stages. The first stage, occurring at a higher temperature, originates from a stress-induced instability [1,2]. It involves mass transport over the whole surface, forming stress-domain structures with a universal optimal periodicity and facet width (domain population) that minimize the surface strain energy. The second stage, occurring at a lower temperature, is dominated by energy difference in facets with different facet angles. It involves mass transport over a shorter range within each period defined in the first step, forming the lowest-energy facet.

Using scanning tunneling microscopy (STM), we investigate the faceting behavior of Si(111) surfaces miscut toward the $[\bar{2}11]$ direction over a wide range of miscut angles from 0.3° to 6°. The surfaces are cleaned by a standard procedure: degassing at 700 °C for several hours in a vacuum chamber (base pressure 2×10^{-10} torr) followed by heating a few times to 1250 °C for ~10 sec each. The cleaned surfaces are then annealed at 950 °C for a few minutes followed by slow cooling to room temperature at a rate of 1 °C/sec. The slow cooling rate is found critical to obtain the well-ordered surface patterns and low defect density in the (7×7) reconstructed terraces. The surface structure remained unchanged if the cooling rate is much slower than 1 °C/sec. For each miscut a large number of STM images are acquired from different Si(111) samples and from different cleaning-annealing cycles.

Figure 1 shows STM images of four typical ordered patterns formed on surfaces with a miscut angle of 1°, 2°, 4°, and 6°, respectively, consisting of a periodic array of alternating (7 × 7) terraces and step-bunched facets. To quantitatively characterize the length scales of the patterns, the periodicity (terrace width + facet width) and the facet width are measured separately as a function of the miscut angle, as shown in Figs. 2a and 2b, respectively. The value for a given miscut angle is derived from the peak position of the Gaussian distribution fit to the experimental data, as shown in the inset of Fig. 2a, demonstrating the preferred periodicity and good degree of long-range order. The measured periodicities are 673, 593, 612, and 662 Å at miscut angles of to 1°, 2°, 4°, and 6°, respectively, with an average value of 635 Å.

All the patterns have the same periodicity independent of the miscut angle (Fig. 2a), while the facet width increases linearly with increasing miscut (Fig. 2b). Such a length-scale relationship implies that the facet in all the patterns must have the same facet angle, i.e., facet structure. This is indeed confirmed by high-resolution STM images of the facet, as shown in Fig. 3. The detailed atomic structure of the miniterraces in a facet appears disordered, and all the facets have an average step-step separation of 28 Å and a step height of 6.3 Å, amounting to a facet angle of 12.7°. The 6.3 Å equals a double bilayer step height in Si(111), so a transition from a single bilayer step to a double bilayer step must have occurred in addition to the bunching of steps during faceting. The length-scale relationship also independently verifies the existence of a preferred periodicity
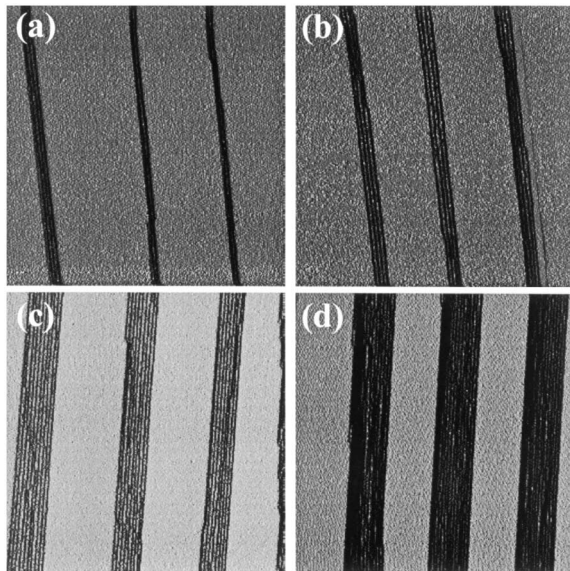
since the surface miscut has to be preserved after faceting. The same facet structure seems to be a special feature associated with azimuthal orientation of the $[\bar{2}11]$ direction. If the Si(111) surface is miscut toward other directions, different facets usually form at different miscut angles [5].

We believe that these unique self-organized length-scale features originate from a faceting transition in which surface stress plays an important role in addition to surface (facet) energy [3]. We propose that the periodicity and facet width are determined, respectively, by minimization of elastic energy and facet energy at two different stages in the transition. Figure 4 shows schematically such a two-stage faceting transition. At a temperature above transition, the surface consists of a staircase of (1 × 1) terraces separated by double bilayer steps (Fig. 4a). As temperature is lowered below the transition temperature, the surface starts nucleation of individual domains of the reconstructed (7 × 7) terraces and then self-organizes into a periodic stress-domain structure [1,2], consisting of alternating (7 × 7) terraces and step-bunched (1 × 1) terraces (facets) (Fig. 4b). The change of total surface free energy per unit area is

$$\Delta F(T, L, l) = \Delta f(T)\left(1 - \frac{l}{L}\right)$$
$$- \frac{c}{L} \ln\left[\frac{L}{\pi a}\sin\left(\frac{l}{L}\pi\right)\right] + \frac{2\gamma}{L}, \quad (1)$$

FIG. 1. Ordered patterns on Si(111) surfaces. Surface morphology of four well-annealed Si(111) samples with miscut angles of 1°, 2°, 4°, and 6° toward $[\bar{2}11]$ direction are shown. The surfaces display an ordered pattern consisting of alternating (7 × 7) reconstructed terraces and high step-density facets. All four images have the same size of 2400 Å × 2400 Å. The downstairs direction runs from left to right. The derivative mode is used to emphasize the step structure in the facet.
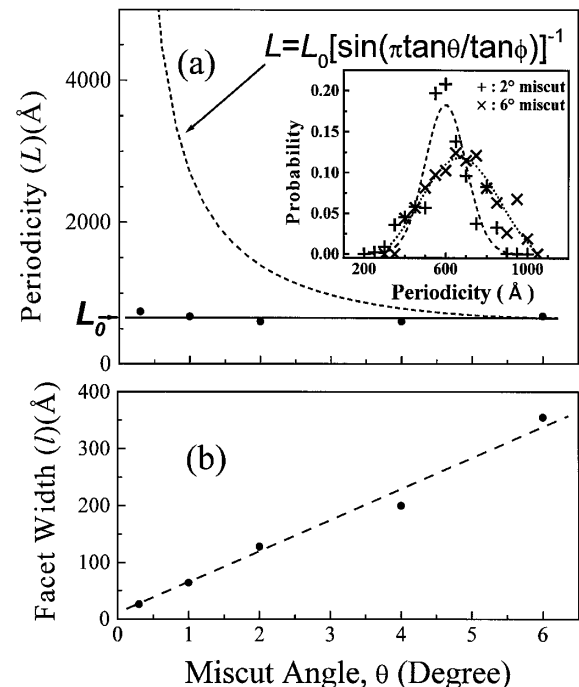

FIG. 2. Dependence of faceting periodicity and facet width on a miscut angle. (a) All ordered patterns adopt a universal periodicity of ~635 Å, independent of miscut angle. Values (dots) for different miscuts are obtained from the peak positions of Gaussian fits to the measured data, as shown in the inset for 2° and 6° samples. The dashed line shows the dependence of periodicity on a miscut angle if a one-stage faceting transition had occurred. (b) The facet width increases linearly with increasing miscut angle. The straight line is a least-squares fit to the data (dots).
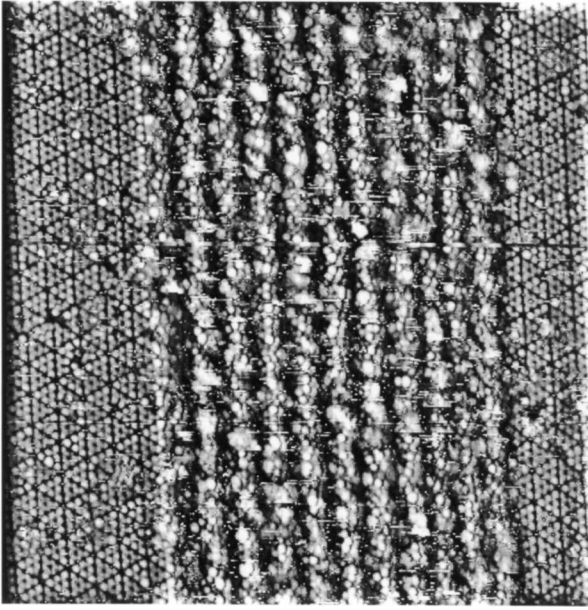
FIG. 3. A typical high resolution STM image of a stable facet. The downstairs direction runs from left to right. Note that the (7×7) terraces terminate at the corner holes at both upper and lower edges of the facet.
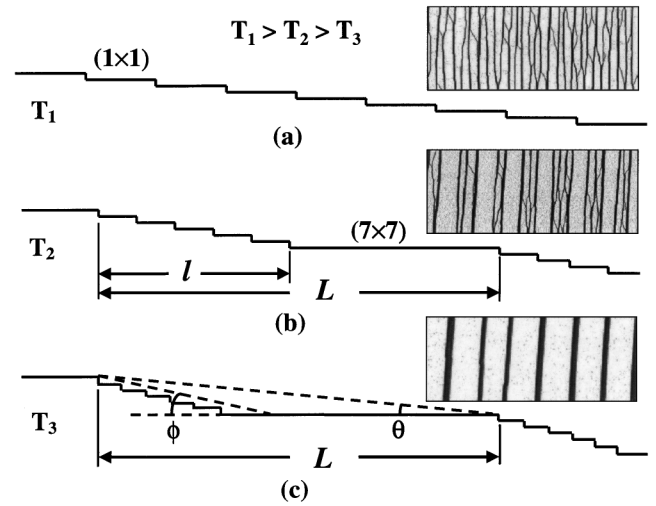

FIG. 4. Schematic illustration and STM demonstration of the two-stage faceting transition. (a) The surface morphology above the faceting transition temperature, consisting of equally spaced double bilayer steps. (b) A half-filled stress-domain structure formed via the first stage, consisting of alternating (7×7) reconstructed terraces and incomplete step-bunched facets. L is the faceting period and $l = L/2$ is the facet width. (c) The final stable morphology, formed via the second stage, consisting of the stable facet with a facet angle of $\phi = 12.7°$. θ is the surface miscut angle. The corresponding STM images show the surface morphology quenched at different stages of the transition from a $2°$ sample. All three images have the size of $0.2 \ \mu m \times 0.5 \ \mu m$.

where T is the temperature, L is the periodicity, l is the facet width, $\Delta f(T) = f_{(7 \times 7)} - f_{(1 \times 1)}$ is the energy difference of the reconstructed (7×7) and the unreconstructed (1×1) terraces, c is a constant related to the difference of surface stress between the (7×7) terrace and the step-bunched facet and elastic constants, γ is the energy cost forming the edge of the facet, and a is a cutoff constant on the order of the (7×7) unit-cell lattice constant.

Minimization of $\Delta F(T, L, l)$ with respect to both L and l leads to

$$\Delta f(T) = -\frac{\pi c}{L} \cot\left(\frac{l}{L} \pi\right), \qquad (2)$$

and

$$L = \pi a_0 \left[\sin\left(\frac{l}{L} \pi\right) \right]^{-1}, \qquad (3)$$

where $a_0 = a \exp[1 + (2\gamma/c)]$. Equations (2) and (3) define the conditions and the length scales of the stress domains. $\Delta f(T)$ decreases with decreasing temperature; it is positive above the (1×1)-to-(7×7) thermodynamic phase transition temperature and negative below. The elastic relaxation drives the individual (7×7) terrace of finite size to nucleate at a temperature where $\Delta f(T) = c/(L - l)$ [3], above the (1×1)-to-(7×7) thermodynamic phase transition temperature where $\Delta f(T)$ vanishes. The ordering occurs at the lower temperatures defined by Eq. (2). Interestingly, the ordering actually starts at a temperature coinciding with the thermodynamic phase transition temperature, forming a domain structure with an optimal half-filled domain population, $l = L/2$ [1]. Correspondingly, from Eq. (3), the domain adopts a periodicity of $L_0 = \pi a_0$, independent of a miscut angle.

Taking surface stress values of $0.1855 \ eV/Å^2$ [11] and $-0.039 \ eV/Å^2$ [12] for the (7×7) and the (1×1) terraces, respectively, and $a = 47 \ Å$, we estimate, from the observed periodicity ($L_0 = 635 \ Å$), a facet edge energy to be $\sim 0.0035 \ eV/Å$. Since the facet edge is formed by converting a (1×1) step into a (7×7) step, this value is compared with the step free energy difference of $\sim 0.004 \ eV/Å$ [4] between a (7×7) step and a (1×1) step, which is determined independently from step meandering measurements. The good agreement provides a quantitative support of the proposed model.

As the temperature is lowered further, $\Delta f(T)$ becomes negative and continues to decrease. Consequently, the (7×7) terraces in every period increase their sizes, decreasing l while maintaining the periodicity L_0, to reduce the surface energy at the expense of the elastic energy. It proceeds until the most favorable facet structure is formed with a facet angle of $12.7°$, as shown in Fig. 4c. Because the same facet structure with identical periodicity is formed in all surface patterns, it is mandatory for the facet width to increase linearly with miscut angle, as shown in Fig. 2b.

The existence of two transition stages is further confirmed by the following experiment. We first slowly cool the surfaces down to a given temperature, and then rapidly quench them to low temperature, to reveal the surface morphology frozen in at different temperatures. The STM images in Fig. 4 show three typical morphologies quenched from above and below the faceting transition temperatures. The surface quenched from above the

transition temperature (Fig. 4a) consists of an array of mostly double steps without facets. The surface quenched from a temperature below the first transition but above the second transition (Fig. 4b) consists of a faceted periodic structure. It has the same universal periodicity as in the ideally faceted surface (Fig. 4c) but imperfect facets; the overall width of the facets is one-half of the periodicity. These indicate that the faceting transition has completed the first stage, defining the optimal periodicity with a half-filled domain structure, but not the second stage. The fast quenching in the second stage makes the second transition, i.e., formation of the stable facet, incomplete. These images also confirm that the faceting transition is accompanied by a single-to-double bilayer step transition.

There are other arguments that support the conclusion of the two-stage faceting transition. If the final ordered patterns were formed directly without the first stage, energy minimization with respect to periodicity (L) under the constraint of constant facet angle ($\phi = 12.7°$) would lead to the following relationship of periodicity and miscut angle (θ), $L_0 = \pi a_0 \{\sin[(\tan\theta / \tan\phi)\pi]\}^{-1}$. Consequently, the periodicity would decrease drastically with increasing miscut angle, as shown in Fig. 2a.

In addition to nucleation and growth, the faceting kinetics of Si(111) has been suggested to involve a spinodal [3], which may also influence the pattern formation. However, if the periodicity (wavelength) were set by a spinodal, it would depend on miscut angle, i.e., step density (equivalent to alloy concentration in classical spinodal theory [13]). In contrast, we observe a universal periodicity, independent of miscut angle. Also, a spinodal pattern would continue to coarsen with time, because it is kinetically selected, while the observed patterns remain unchanged as long as the cooling rate is slow ($<1 °C/sec$), indicating that they are thermodynamically stable.

One more notable structural feature of the patterns is that the widths of terrace and of facet are quantized, being, respectively, a multiple of m times the size of (7×7) unit cell and n times the width of the miniterrace in facet. [The (7×7) terraces end at the corner hole of the (7×7) reconstruction at both the upper and lower edges of the facet, as shown in Fig. 3.] Consequently, the ratio of m over n is fixed for a given miscut. However, such geometry constraints due to reconstruction frustration [14] do not uniquely choose the respective values of m and n, so they cannot lead to the long-range ordering with a universal periodicity. The constraints do help improve the degree of order by narrowing the terrace width distribution and suppressing kink excitation along the steps [5], as they restrict the deviation of the terrace width from its preferred value in multiple units of (7×7) unit cell.

In conclusion, we have demonstrated self-organized pattern formation on Si(111) surfaces with miscuts toward the $[\bar{2}11]$ direction. The patterns consist of a periodic array of alternating (7×7) reconstructed terraces and high-step-density facets. Most importantly, the length scales of the patterns can be controlled by a universal periodicity and a facet width that increases linearly with increasing miscut. Such well-ordered patterns may be used as templates for subsequent nanofabrication. We propose a two-stage faceting transition model to explain the self-organization process. The first stage, dominated by minimization of the elastic energy, defines the universal periodicity; the second, dominated by minimization of the facet energy, creates a common facet structure and controls the facet width.

*Corresponding author.
Email address: phymen@ccunix.ccu.edu.tw

[1] V. I. Marchenko, JETP Lett. **33**, 381 (1981); O. L. Alerhand, D. Vanderbilt, R. D. Meade, and J. D. Joannopoulos, Phys. Rev. Lett. **61**, 1973 (1988).

[2] F. K. Men, W. E. Packard, and M. B. Webb, Phys. Rev. Lett. **61**, 2469 (1988); M. B. Webb, F. K. Men, B. S. Swartzentruber, R. Kariotis, and M. G. Lagally, Surf. Sci. **242**, 23 (1991).

[3] R. J. Phaneuf, N. C. Bartelt, E. D. Williams, W. Swiech, and E. Bauer, Phys. Rev. Lett. **67**, 2986 (1991); R. J. Phaneuf, N. C. Bartelt, and E. D. Williams, Phys. Rev. Lett. **71**, 2284 (1993).

[4] E. D. Williams, R. J. Phaneuf, J. Wei, N. C. Bartelt, and T. L. Einstein, Surf. Sci. **294**, 219 (1993).

[5] H. Hibino, T. Fukuda, M. Suzuki, Y. Homma, T. Sato, M. Iwatsuki, K. Miki, and H. Tokumoto, Phys. Rev. B **47**, 13 027 (1993); J.-L. Lin, D. Y. Petrovykh, J. Viernow, F. K. Men, D. J. Seo, and F. J. Himpsel, J. Appl. Phys. **84**, 255 (1998).

[6] M. Kasu and N. Kobayashi, Appl. Phys. Lett. **62**, 1262 (1993).

[7] S. Rousset, F. Pourmir, J. M. Berroir, J. Klein, J. Lecoeur, P. Hecquet, and B. Salanon, Surf. Sci. **422**, 33 (1999).

[8] G. M. Watson, Doon Gibbs, D. M. Zehner, Mirang Yoon, and S. G. J. Mochrie, Phys. Rev. Lett. **71**, 3166 (1993).

[9] P. E. Wierenga, J. A. Kubby, and J. E. Griffith, Phys. Rev. Lett. **59**, 2169 (1987).

[10] O. L. Alerhand, A. N. Berker, J. D. Joannopoulos, D. Vanderbilt, R. J. Hamers, and J. E. Demuth, Phys. Rev. Lett. **64**, 2406 (1990).

[11] R. E. Martinez, W. M. Augustyniak, and J. A. Golovchenko, Phys. Rev. Lett. **64**, 1035 (1990).

[12] D. Vanderbilt, Phys. Rev. Lett. **59**, 1456 (1987).

[13] J. W. Chan, Trans. Metall. Soc. AIME **242**, 167 (1968).

[14] L. Leprince, F. Houzay, and J. M. Moison, Phys. Rev. B **48**, 14 683 (1993).